the expansion: we find that $L_i \approx 10^{11}$ m^{-2}. This is a conservative estimate in that the experimental error leads to an upper bound that is larger by several orders of magnitude, and a lower bound of 5×10^{10} m^{-2}. Although more accurate values of L_i will be obtained when the sensitivity of the electronics to mechanical shock has been reduced, it is already clear that the density of vortices generated is very large. To put these figures into perspective, note that the production of a line density of $\sim 10^{11}$ m^{-2} by rotation[5] of a vessel of liquid ^{4}He would require an angular velocity of $\sim$4,000 rad s^{-1}, an enormous value.

This copious production of vortices created, as predicted[2,3], by passage through the λ-transition implies, by analogy, that cosmic strings were generated in the mathematically similar second-order phase transition of the early Universe, and that they would therefore have been avilable to play the role in galaxy formation proposed by Kibble[1]. □

Received 20 December 1993; accepted 18 February 1994.

1. Kibble, T. W. B. *J. Phys.* A**9,** 1387–1398 (1976).
2. Zurek, W. H., *Nature* **317,** 505–508 (1985).
3. Zurek, W. H. *Acta phys. pol.* B**24,** 1301–1311 (1993).
4. Kibble, T. W. B. *Nature* **317,** 472 (1985).
5. Donnelly, R. J. *Quantized Vortices in Helium II* (Cambridge Univ. Press, 1991).
6. Tilley, D. R. & Tilley, J. *Superfluidity and Superconductivity* 2nd edn (Hilger, Bristol, 1986).
7. Ginzburg, V. L. & Pitaevskii, L. P. *Soviet Phys. JETP* **7,** 858–861 (1958).
8. Vilenkin, A. *Phys. Rep.* **121,** 263–315 (1985).
9. Chuang, I., Turok, N. & Yurke, B. *Phys. Rev Lett.* **66,** 2472–2475 (1991).
10. Bowick, M. J., Chander, L., Schiff, E. A. & Srivastava, A. M. *Science* **263,** 943–945 (1994).
11. Hendry, P. C. & McClintock, P. V. E. *Cryogenics* **27,** 131–138 (1987).
12. Wilks, J. *The Properties of Liquid and Solid Helium* (Clarendon Press, Oxford, 1967).
13. Williams, G. A. *J. Low Temp. Phys.* **89,** 91–100 (1992).
14. Vinen, W. F. *Proc. R. Soc.* A**242** 493–515 (1957).
15. Schwarz, K. W. & Rozen, J. R. *Phys. Rev. Lett.* **66,** 1898–1901 (1991).
16. Smith, M. R., Donnelly, R. J., Goldenfeld, N. & Vinen, W. F. *Phys. Rev. Lett.* **71,** 2583–2586 (1993).

ACKNOWLEDGEMENTS. Discussions with D. H. Lyth, H. J. Maris, E. N. Smith, W. F. Vinen, G. A. Williams and W. H. Zurek are acknowledged. The research is supported by the UK Science and Engineering Research Council.

Generalized synthesis of periodic surfactant/inorganic composite materials

Qisheng Huo*, David I. Margolese*, Ulrike Ciesla†, Pingyun Feng*, Thurman E. Gier*, Peter Sieger*, Rosa Leon‡, Pierre M. Petroff‡, Ferdi Schüth§ & Galen D. Stucky*§

* Department of Chemistry, University of California, Santa Barbara, California 93106, USA
† Institut für Anorganische Chemie, Johannes-Gutenberg Universität, 55099 Mainz, Germany
‡ Center for Quantized Electronic Structures, University of California, Santa Barbara, California 93106, USA

THE recent synthesis of silica-based mesoporous materials[1,2] by the cooperative assembly of periodic inorganic and surfactant-based structures has attracted great interest because it extends the range of molecular-sieve materials into the very-large-pore regime. If the synthetic approach can be generalized to transition-metal oxide mesostructures, the resulting nanocomposite materials might find applications in electrochromic or solid-electrolyte devices[3,4], as high-surface-area redox catalysts[5] and as substrates for biochemical separations. We have proposed recently[6] that the matching of charge density at the surfactant/inorganic interfaces governs the assembly process; such co-organization of organic and inorganic phases is thought to be a key aspect of biomineralization[7]. Here we report a generalized approach to the synthesis of periodic mesophases of metal oxides and cationic or anionic surfactants under a range of pH conditions. We suggest that the assembly process is controlled by electrostatic complementarity between the inorganic ions in solution, the charged surfactant head groups and—when these charges both have the same sign—inorganic counterions. We identify a number of different general strategies for obtaining a variety of ordered composite materials.

Four pathways to the synthesis of mesostructured surfactant-inorganic biphase arrays are depicted in Fig. 1. Route 1 involves the direct co-condensation of anionic inorganic species with a cationic surfactant (S^+I^-); the syntheses of MCM-41 and MCM-48 (refs 1, 2) are prototypic examples. We have now found a similar route to periodic tubular non-silica structures, but involving cooperative condensation of a cationic inorganic species with an anionic surfactant (S^-I^+), (route 2) a possibility predicted in ref. 6. By contrast, routes 3 and 4 involve condensation of ionic inorganic species in the presence of similarly charged surfactant molecules. These pathways are mediated by counterions of opposite charge to that of the surfactant head group (solution species ($S^+X^-I^+$) where $X^- = Cl^-$, Br^-; or, ($S^-M^+I^-$) where $M^+ = Na^+$, K^+).

Lamellar, MCM-41 and MCM-48 periodic porous silicates (S^+I^-) are obtained under basic conditions by the self-assembly of anionic silicates and cationic surfactant molecules[1,2,6,8]. We suggested in ref. 6 that this mechanism should work for other oxides as well, if the pH is varied to adjust the charge density of the metal oxide polyanions. Thus, we were able to synthesize lamellar tungsten (VI) oxide ($d_{100} = 31$ Å, where d_{100} is the first X-ray diffraction line) at pH above 8, and lamellar and hexagonal tungsten (VI) oxide phases ($d_{100} = 40$ Å) at pH 4–8 (Fig. 2) using cationic surfactants. As another example, both cubic (*Ia*3*d*, pH 6.5–7.0) and hexagonal (pH 6.0–6.5) antimony (V) oxide mesostructures were synthesized in lower-pH windows for the anionic inorganic phase. By choosing inorganic species (for example, antimony or tungsten oxides) that are more acidic than silicic acid, the cooperative biphase templating can be carried out at neutral and lower pH values to obtain a match of the charge density of the oxide to that of the respective surfactant phase.

A similar approach was taken in a charge-reversed situation, where an anionic surfactant was used to direct the condensation of cationic oxide species (S^-I^+). $C_{16}H_{33}SO_3H$ was used in the synthesis of iron and lead oxides, giving a hexagonal phase ($d_{100} = 45.8$ Å for Pb) and different lamellar phases (for example, 38.5 Å for Pb and 41.0 Å for Fe). Lamellar phases were obtained depending on the synthesis conditions (pH 1–5), using oxides of Mg, Al, Mn, Fe, Co, Ni and Zn with $C_{12}H_{25}PO_4H_2$ as the surfactant. An interesting example is aluminium oxide with sodium dodecylbenzenesulphonate at 70 °C and pH 3.5, which slowly rearranges to increase the layer spacing (28.9 to 32.1 Å in 8 hours to 9 days). It should be noted that the anionic polar head group can be a part of the inorganic framework in these materials.

Surprisingly, the formation of mesophases was possible by the cooperative assembly of cationic inorganic species with cationic surfactants. Generally lamellar, hexagonal and *Pm*3*n* cubic phases (Fig. 1) were prepared by addition of tetraethyl-orthosilicate (TEOS) at room temperature to an acidic (for example, HCl) solution of surfactant. After stirring for 30 min or longer, the solid product was recovered by filtration and studied by X-ray diffraction and high-resolution transmission electron micros-

§ To whom correspondence should be addressed.

copy (Figs 2, 3). High-quality samples of the three phases can be formed in a wide range of strongly acidic conditions (1–7 M HCl or HBr). We found that HCl favours the formation of all three phases, whereas HBr favours the formation of the hexagonal and not the cubic phase. In contrast to the synthesis conditions used previously[1,2,6] for M41S silicate mesophases, extremely acidic media, low temperatures, short synthesis times and low concentrations of surfactant were employed. Zwitterionic and lipid-like surfactants were successfully used in this synthesis. Silica polymerization proceeds in this pH range through the condensation of cationic intermediates[9,10].

The new cubic silica phase, first reported here (Figs 1–3), was prepared using surfactants with larger head groups (for example, alkyltriethylammonium, cetylethylpiperidinium) as the template. This was done to decrease the value of the surfactant packing parameter to generate maximum surface curvature[11,12]. The X-ray diffraction data closely matches (intensities and indexing) that for the I_1 ($Pm3n$) phase of cetyltrimethylammonium chloride and cetylpyridinium chloride in formamide[13]. This phase consists of a packing of two types of discrete micellar aggregates[13–17] in globular-like cages, with one large cage of ~30 Å diameter giving a clathrasil-like structure. Removal of the $C_{16}TEA^+$ (triethylammonium) template by calcination at 500 °C resulted in a reduction of the unit cell parameter from 89.9 to 78.2 Å.

The surfactant–silica mesophases exhibit different unit cell parameters when surfactants with differing alkyl chain lengths were used (Fig. 5). Moreover, the X-ray diffraction data (Fig. 5), show clearly that similar surfactants at pH < 0 produce mesostructures with similar, but slightly larger d-spacings than those obtained by basic (pH > 9) medium synthesis. For the $C_{16}TMA^+$ (trimethylammonium) hexagonal phase product formed in acidic media, chemical analysis gave (wt%): SiO_2, 39.7; $C_{16}TMA^+$, 46.38; Cl, 5.75. The product surfactant/Cl ratio is therefore 1.0 : 1.0, a feature that distinguishes these mesostructure phases from hexagonal phase MCM-41 formed in alkaline solution which has no significant halide content using the same surfactant halide starting materials. Because in the acid mesophase product the template cationic charge is exactly balanced by a halide anion, the template should be removable without providing an exchangeable cation, as required for the anionic frameworks of MCM-41 (ref. 18). Indeed, it was found that >85% of the template could be removed from the material as-synthesized by stirring in pure ethanol at room temperature or by overnight reflux. The removal of the template was also possible by calcination. The calcined hexagonal phases (at 500 °C) had surface areas greater than 1,000 $m^2 g^{-1}$ and average pore diameters of 18.6, 26.5 and 33.2 Å for C_{14}, C_{16} and C_{18} TMA^+, respectively, as determined by N_2 BET (Brunauer–Emmett–Teller) measurements.

^{29}Si MAS (magic angle spinning) NMR data (Fig. 4) were used to determine the degree of polymerization and the concentration of silanol, as measured by the ratio of the two major peaks (denoted Q^3 and Q^4). At long reaction times, for the hexagonal phase, Q^3/Q^4 decreases due to increased polymerization, but for a given reaction time, Q^3/Q^4 is approximately the same (0.55) as for the hexagonal material precipitated from basic medium.

As proposed for the co-condensation of oligomeric polysilicate and cationic surfactant molecules in alkaline solution (pH > 9)[1,2,6], we believe that the main driving force for self-assembly in strong acid media is electrostatic. We postulate that

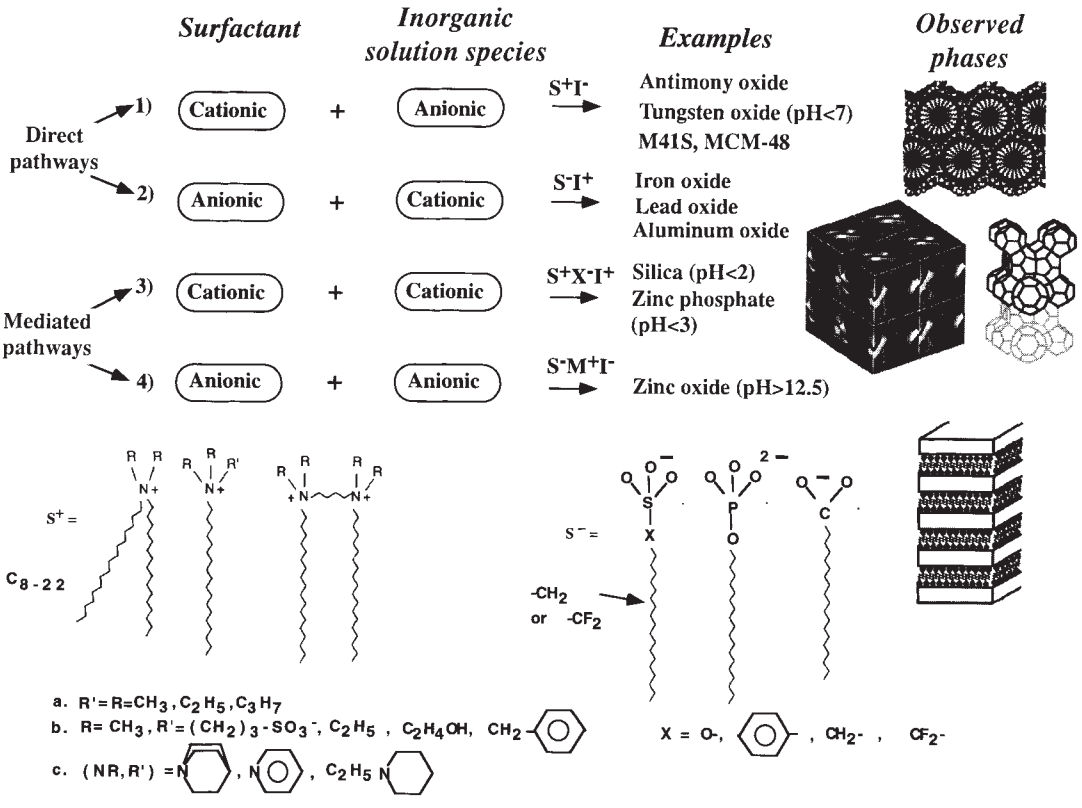

FIG. 1 A general scheme for the self-assembly reaction of different surfactant and inorganic species. The mesostructured phases can be synthesized by either direct pathways or mediated pathways, using different charged surfactant molecules and inorganic solution species in certain pH conditions. Some surfactants other than alkyltrimethylammonium ions are also good templates for mesoporous materials syntheses. Each surfactant can act as a template for the formation of one or more mesostructures in different reaction conditions. The topology of the composite mesostructures reflects the final geometry adopted by the organized organic array so that regardless of the inorganic framework composition, liquid-crystal morphologies have been observed and can be expected. The dimensionless effective surfactant packing parameter $g = V/a_0 l$ determines the product structure[11,12,25], where V is the chain volume, l is the chain length and a_0 is the optimum head-group area of a surfactant molecule.

the interactions between cationic silica species and halide-cationic surfactant headgroups are mediated by the halide ions, which form hydrogen bonds to protonated silanols such as $\equiv Si(OH_2)^+$ (ref. 10). At high concentrations of hydrogen halide solutions, the cationic surfactant hydrophilic region is surrounded by halide ions forming an electrical double layer (S^+X^-) with the periphery negatively charged. As cooperative assembly and precipitation proceeds, the protons associated with the silica species along with associated excess halide ions are excluded until a neutral inorganic framework remains.

This model is supported by: (1) the fact that cationic silica species are present at $pH < 2$ (refs 9,10) and the fact that the solution $[H^+]$ does not change during synthesis; (2) the 1 : 1 surfactant to chlorine ratio in the hexagonal product; (3) the easy removal of the template with ethanol; (4) the observation that TEOS and $SiCl_4$ hydrolyse and form mesophase products, whereas Cab-O-Sil (SiO_2) which does not dissociatively hydrolyse in acidic conditions, forms no mesophase products. Clearly the template mechanism for ($S^+X^-I^+$) synthesis is not the same as that for (S^+I^-) synthesis.

We have applied the above approach to the synthesis of organized Zn-containing phosphate mesostructured materials. At least four lamellar $(C_nTMA)^+X^-[HZnPO_4]$ (X is Cl^-, Br^-) phases with different *d*-spacings and surfactant packing, including monolayer and bilayer geometries, can be generated by controlling composition and pH. One of them was formed from solutions containing $[H_2ZnPO_4]^+$ ($pH \sim 2.5$) (Figs 3, 5), and like the acid silica phases contains one halide ion per surfactant molecule. In this structure there is three-dimensional ordering and excellent lateral ordering of layers. Comparison with the

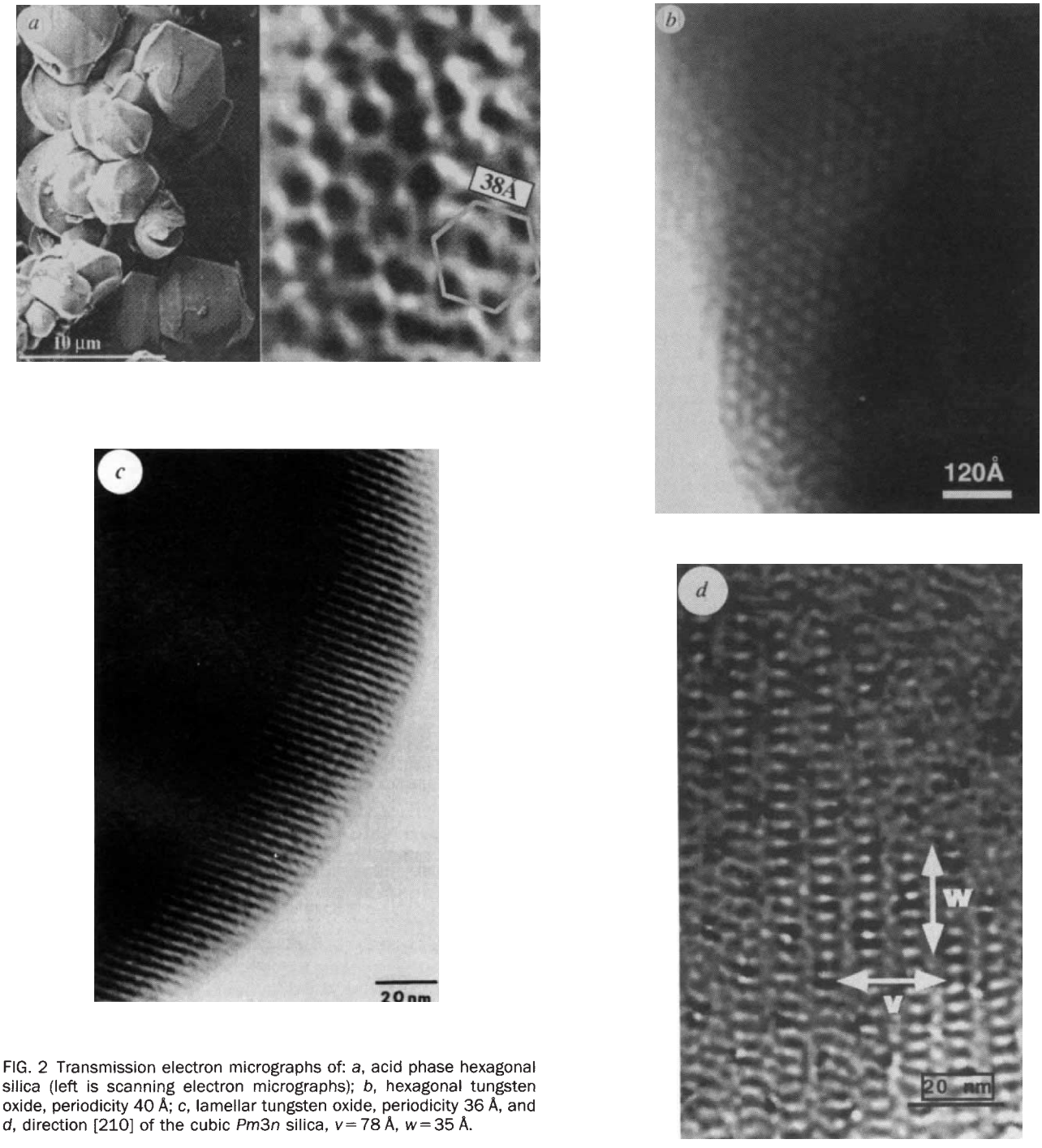

FIG. 2 Transmission electron micrographs of: *a*, acid phase hexagonal silica (left is scanning electron micrographs); *b*, hexagonal tungsten oxide, periodicity 40 Å; *c*, lamellar tungsten oxide, periodicity 36 Å, and *d*, direction [210] of the cubic *Pm3n* silica, $v = 78$ Å, $w = 35$ Å.

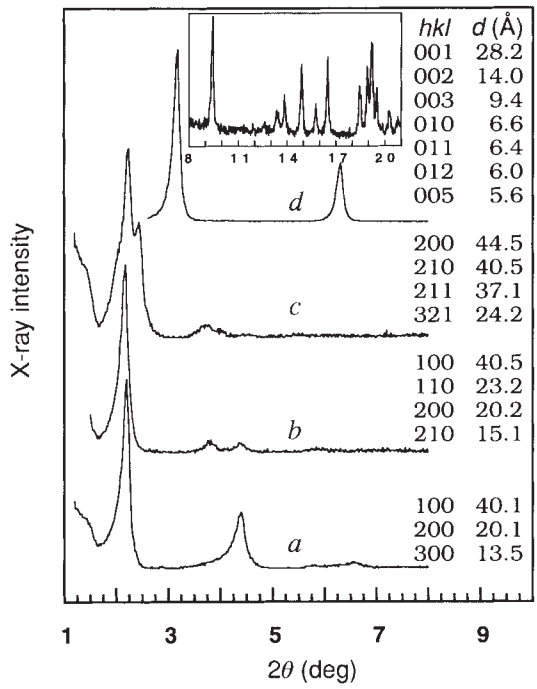

FIG. 3 Powder X-ray diffraction (XRD) patterns of silica and zinc phosphate mesostructures precipitated from acidic medium. From bottom to top, the patterns are: (*a*) lamellar silica, $a_0 = 39.8$ Å; (*b*) hexagonal silica (MCM-41), $a_0 = 47.6$ Å; (*c*) cubic *Pm3n* silica, $a_0 = 89.9$ Å; (*d*) lamellar zinc phosphate, with the high-2θ region shown in the inset. These peaks (*d*) could be indexed in an orthorombic cell having $a = 6.49$ Å, $b = 6.57$ Å and $c = 28.08$ Å. Typical preparation of the silica mesophases from acidic medium was carried out with the following molar ratios: (*a*) lamellar: 0.12 C_{20}TMA-Br:1TEOS:4.9 HCl:130 H_2O; (*b*) hexagonal: 0.12 C_{16}TMA-Br:1 TEOS:9.2 HCl:130 H_2O and (*c*) cubic: 0.13 C_{16}TEA-Br:1 TEOS:10.4 HCl:130 H_2O. The lamellar zinc phosphate phase shown here (*d*) was synthesized by crystallization of a reaction mixture with molar composition of 3.0 $Zn(NO_3)_2$: 3.5 H_3PO_4:5.0 C_{16}TMA-Br:4.5 TMA-OH: 1,000 H_2O at 4 °C for 18 d (pH 2) to give a final composition of $[(C_{16}H_{33})N(CH_3)_3^+Br^-]\cdot HZnPO_4$, [observed, calculated: Zn (12.4%, 12.5%); Br (15.4%, 15.2%); N (2.9%, 2.7%); and P (5.5%, 5.9%)]. By varying pH and dilution, other lamellar structures can be obtained with spacings of 63, 37.3 and 29.7 Å and surfactant chain length to lattice spacing variation which suggests a surfactant bilayer configuration for the first of these. In these lamellar phases, the residue obtained after thermal analysis to 900 °C is $Zn_2P_2O_7$.

determined structures of the layered $MH(ZnPO_4)_2$ (where M is Na, Cs) (ref. 19) strongly supports a template model similar to that for the acid synthesized silica phases, with the cationic surfactant indirectly coordinated to the $HZnPO_4$ walls by hydrogen bonding to the anion (Cl^- or Br^-).

Finally, we have explored the possibility of synthesizing periodic biphase arrays from negatively charged surfactants and inorganic species (S^-I^-). For instance, $Zn(OH)_3^-$, $Zn(OH)_4^{2-}$ and $Zn_2(OH)_6^{2-}$ are the predominant species in a 0.1 M solution of ZnO (pH 10–14) (ref. 20). The anionic surfactant $CH_3(CH_2)_{16}COO^-M^+$ gives a lamellar zinc oxide phase (d_{001} = 48.8 Å, 50.3 Å; $M^+ = Na^+$, K^+, respectively) above pH 12.5 (TMA-OH without surfactant under the same reaction conditions gives only ZnO), consistent with a mediated templating ($S^-M^+I^-$) pathway. Anionic surfactants compete with oxide/hydroxide groups for framework metal atom coordination sites and under similar conditions phosphates such as $C_{12}H_{25}OPO_3Na_{2-x}H_x$ ($x = 0$–1) appear to coordinate directly to the zinc atom, thus becoming part of the framework with no sodium ions present in the final product. In another example, at pH >8 using an anionic aluminate species in solution lamellar ($d_{001} = 33.6$ Å) $[C_{12}H_{25}OPO_3NaH]_3\cdot Al(OH)_3\cdot 4H_2O$ (observed and calculated Al (2.5%, 2.5%); P (8.6%, 8.6%); C (40.2%, 39.7%); H (7.7%, 8.9%); Na (5.56%, 6.35%)) is formed in contrast to lamellar $[C_{12}H_{25}OPO_3]\cdot Al(OH)\cdot 2H_2O$ (observed and calculated Al (7.9%, 8.2%); P (9.3%, 9.5%); C (44.4%, 44.2%); H (8.6%, 8.6%)) which forms at pH <5. The former is consistent with a ($S^-M^+I^-$) solution pathway and no framework phosphate, whereas in the latter the (S^-I^+) chemistry prevails with surfactant framework participation.

The results presented here confirm the feasibility of using the synergistic interface chemistry of inorganic and organic species to create periodic mesostructures with cationic or anionic inorganic species including transition-metal oxides and cationic or anionic surfactants. A variety of surfactants including lipids and zwitterionic types were used so that this chemistry becomes directly applicable to biomimetics. Our periodic biphasic arrays are to be contrasted with the tubules of silica[21] and iron oxide[22] grown on a charged lipid template. Charge matching of the biphasic arrays can be accomplished through the four pathways shown in Fig. 1. but even these may not be exclusive as charge

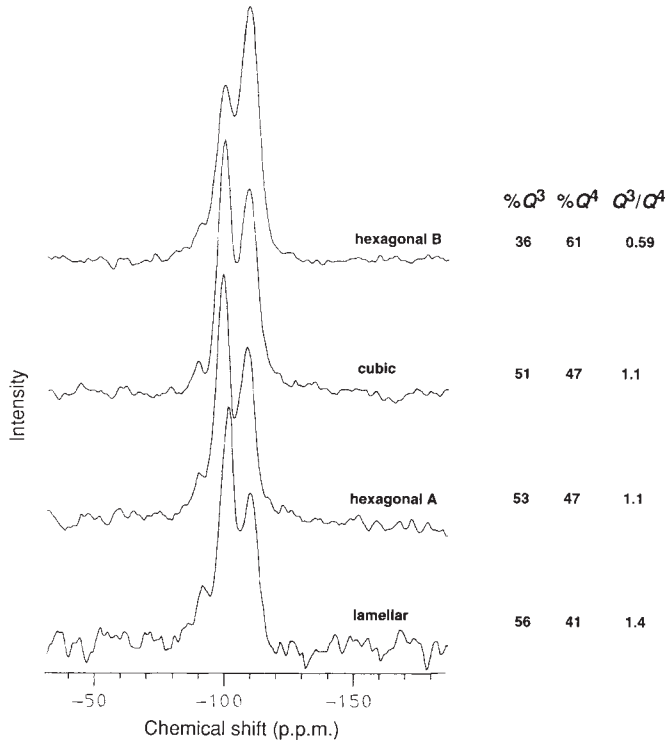

FIG. 4 ^{29}Si MAS NMR of the as-synthesized silica mesophases. For all four of the materials the two major peaks shown are Q^3 (at −101 to −102 p.p.m.) and Q^4 (at −110 to −111 p.p.m.) (ref. 26). $\%Q^3$ measures the number of ^{29}Si of the type $(SiO)_3{\equiv}\underline{Si}{-}OH$ and $\%Q^4$ measures the number of ^{29}Si of the type $(SiO)_3{\equiv}\underline{Si}{-}O{-}\underline{Si}{\equiv}$. The estimated error in the values of Q^3 and Q^4 are ±5% of their value. Hexagonal phase A was run at short reaction time (30 min) and hexagonal phase B was run under the same synthesis conditions except for long reaction time (2 h). The Q^3/Q^4 ratio measures the extent of silanol condensation indicating for material B a more condensed framework than material A. Q^3/Q^4 for the hexagonal phase and for the lamellar phase in acidic media is similar to that found for materials precipitated from basic media, which are 0.55 and 1.2 respectively. Chemical shifts were measured with respect to tetramethylsilane.

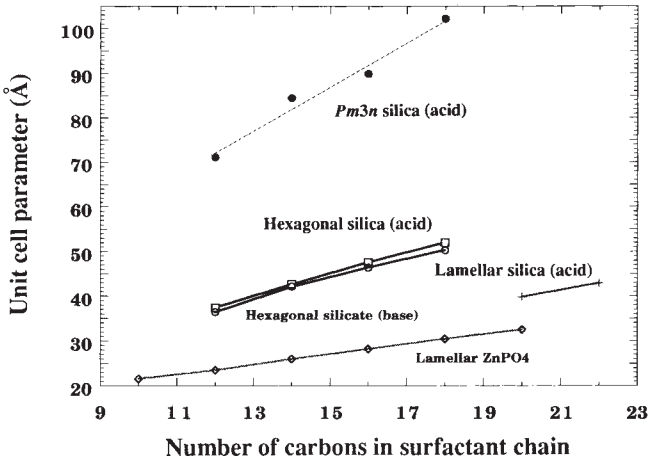

FIG. 5 The relationship between unit cell parameter and number of carbon atoms in surfactant chain. Silica (*Pm3n*) phase was synthesized by using alkyltriethylammonium as template at room temperature for 1 h. Hexagonal silica and silicate phases were obtained in the presence of alkyltrimethylammonium at room temperature in acidic and basic media respectively. Only $C_{20-22}TMA^+$ led to the formation of lamellar silica in acidic medium at room temperature. Lamellar $ZnPO_4$ was prepared by using alkyltrimethylammonium as template from acidic medium (pH 2.5). Estimated error is 1 Å in *d*-spacing of highest peak (d_{210} for *Pm3n* phase and d_{100} for hexagonal and lamellar phases).

matching also might be accomplished through a combination of both direct and mediated linkages. Ultimately, temporal and spatial control of the relative rates of the biphase and interface assembly processes in cooperative templating might be used to impose microscopic long-range modulation of the periodic compositive array morphology in a manner directly relevant to biomaterial synthesis[23,24]. □

Received 21 September 1993; accepted 27 January 1994.

1. Kresge, C. T., Leonowicz, M. E., Roth, W. J., Vartuli, J. C. & Beck, J. S. *Nature* **359,** 710–712 (1992).
2. Beck, J. S. *et al. J. Am. chem. Soc.* **114,** 10834–10843 (1992).
3. Lampert, C. M. & Granqvist, C. G. in *Large-Area Chromogenics: Materials and Devices for Transmittance Control* (eds Lampert, C. M. & Granqvist, C. G.) 2–19 (SPIE Optical Engineering, Washington DC, 1990).
4. Dautremont-Smith, W. C. *Displays* **3,** 3–22 (1982).
5. Parton, R. F., Jacobs, J. M., van Ooteghem, H. & Jacobs, P. A. *Zeolites as Catalysts, Sorbents and Detergent Builders* (eds Karge, H. G. & Weitkamp, J.) 211–212 (Elsevier, Amsterdam, 1989).
6. Monnier, A. *et al. Science* **261,** 1299–1303 (1993).
7. Mann, S. *Nature* **365,** 499–505 (1993).
8. Inagaki, S., Fukushima, Y. & Kuroda, K. *J. chem. Soc., chem Commun.* 680–682 (1993).
9. Iler, R. K. *The Chemistry of Silica* (Wiley, New York, 1979).
10. Brinker, C. J. & Scherer, G. W. *Sol-Gel Science* 97–233 (Academic, San Diego, 1990).
11. Hyde, S. T. *Pure appl. Chem.* **64,** 1617–1622 (1992).
12. Israelachvili, J. N., Mitchell, D. J. & Ninham, B. W. *J. chem. Soc., Faraday Trans. 2* **72,** 1525–1568 (1976).
13. Auvray, X. *et al. Langmuir* **9,** 444–448 (1993).
14. Vargas, R., Mariani, P., Gulik, A. & Luzzati, V. *J. molec. Biol.* **225,** 137–145 (1992).
15. Charvolin, J. & Sadoc, *J. F. J. Phys. Paris* **49,** 521–526 (1988).
16. Seddon, J. M. & Templer, R. H. *Phil. Trans. R. Soc.* A**344,** 377–401 (1993).
17. Fontell, K. *Colloid Polym. Sci.* **268,** 264–285 (1990).
18. Whitehurst, D. D. US Patent No. 5143879 (1992).
19. Nenoff, T. M., Harrison, W. T. A., Gier, T. E., Galabrese, J. C. & Stucky, G. D. *J. Solid St. Chem.* **107,** 285–295 (1993).
20. Baes, C. F. Jr & Mesmer, R. E. *The Hydrolysis of Cations* 287–294 (Wiley International, New York, 1976).
21. Barai, S. & Schoen, P. *Chem. Mater.* **5,** 145–147 (1993).
22. Archibald, D. D. & Mann, S. *Nature* **364,** 430–433 (1993).
23. Friedbacher, G., Hansma, P. K., Ramli, E. & Stucky, G. D. *Science* **253,** 1261–1263 (1991).
24. Morse, D. E., Cariolou, M. A., Stucky, G. D. & Hansma, P. *Mat. Res. Soc. Symp. Proc.* **292,** 59–67 (1993).
25. Rosen, M. J. *Surfactants and Interfacial Phenomena* 108–142 (Wiley, New York, 1989).
26. Lippmaa, E., Magi, M., Samoson, A., Engelhardt, G. & Grimmer, A. R. *J. Am. chem. Soc.* **102,** 4889–4893 (1980).

ACKNOWLEDGEMENTS. We thank S. Mann for suggestions and comments. This work was supported by the US Office of Naval Research (G.D.S. and D.I.M.), the US NSF (G.D.S. and Q.H.), Air Products (G.D.S., T.E.G. and Q.H.), DFG (P.S., U.C. and F.S.) and the US NSF Science and Technology Center (R.L. and P.M.F.). We made use of MRL Central Facilities supported by the US NSF.

Titanium-containing mesoporous molecular sieves for catalytic oxidation of aromatic compounds

Peter T. Tanev, Malama Chibwe & Thomas J. Pinnavaia*

Department of Chemistry and Center for Fundamental Materials Research, Michigan State University, East Lansing, Michigan 48824, USA
* To whom correspondence should be addressed

TITANIUM silicalite is an effective molecular-sieve catalyst for the selective oxidation of alkanes, the hydroxylation of phenol and the epoxidation of alkenes in the presence of H_2O_2 (refs 1–3). The range of organic compounds that can be oxidized is greatly limited, however, by the relatively small pore size (about 0.6 nm) of the host framework[4]. Large-pore (mesoporous) silica-based molecular sieves have been prepared recently by Kresge *et al.*[5–7] and Kuroda *et al.*[8]; the former used a templating approach in which the formation of an inorganic mesoporous structure is assisted by self-organization of surfactants, and the latter involved topochemical rearrangement of a layered silica precursor. Here we describe the use of the templating approach to synthesize mesoporous silica-based molecular sieves partly substituted with titanium—large-pore analogues of titanium silicalite. We find that these materials show selective catalytic activity towards the oxidation of 2,6-di-tert-butyl phenol to the corresponding quinone and the conversion of benzene to phenol.

We have prepared hexagonal mesoporous silica (designated HMS) and its titanium-substituted derivative (Ti-HMS) by acid hydrolysis of $Si(OC_2H_5)_4$ or of $Ti(iso\text{-}OC_3H_7)_4$: $Si(OC_2H_5)_4$ mixtures in alcoholic solutions using dodecylamine (DDA) as a template. This preparative strategy differs from all previously

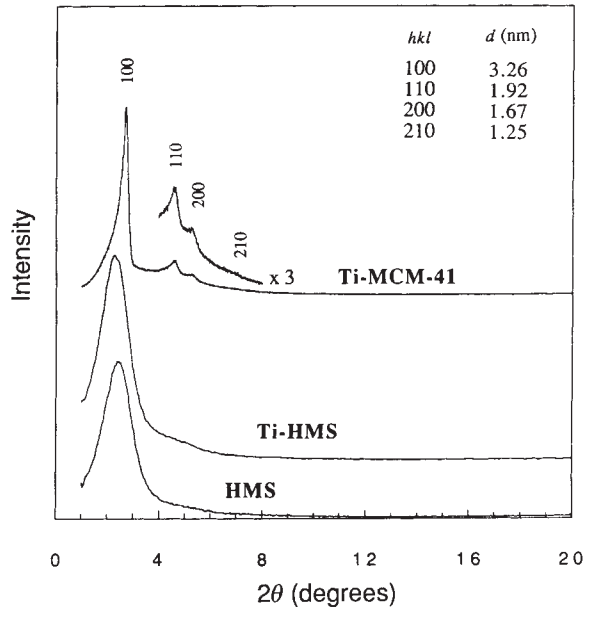

FIG. 1 X-ray powder diffraction patterns of mesoporous molecular sieves. The diffraction patterns were recorded on a Rigaku Rotaflex diffractometer equipped with a rotating anode and using Cu Kα radiation ($\lambda = 0.15418$ nm). The *hkl* and *d* spacing given apply to Ti-MCM-41.